Stanisław BOGDAŃSKI

The Behaviour of Surface Breaking Contact Fatigue Crack in EHL Conditions

Institute of Aeronautics and Applied Mechanics, Warsaw University of Technology, Nowowiejska 24, 00-665 Warsaw, Poland

Keywords: Rolling contact fatigue cracks, elasto-hydro-dynamic lubrication, stress intensity factors,

ABSTRACT: The behaviour of a surface breaking rolling-contact fatigue crack, which is exposed to the elasto-hydro-dynamic lubrication (EHL) conditions is analysed. Fully developed EHL conditions have been assumed, which assure the presence of oil film between the contacting surfaces. This film is assumed to be thick enough to prevent the surface asperities from touching each other. The pressure and traction distributions acting in the oil film obtained from a numerical solution of thermoelastohydrodynamic problem [1] has been taken for the analysis as an approximation of the real load of a crack. Two models of the crack faces interaction have been investigated. The first one assumes the so called "dry conditions", i. e. no liquid, or only small its traces present in the crack interior, and accounts for the tangential and normal interactions between the crack faces. For this case the contact problem for the crack interior has been subsequently solved during cycle of loading. The second approach takes into account penetration of the crack interior by oil, and the presence of a squeeze oil film between the crack faces. The analyses has been performed on the basis of a two - dimensional FE model of a surface breaking, shallow angle crack with the use of EHD and squeeze oil film modelling, through the determination of the values, ranges and histories of variations of the LEFM stress intensity factors; K_I, K_{II} at the crack tip during cyclic EHD contact loading. The results for several angles of crack inclination, and several crack lengths with various values of friction coefficient at the crack faces, as well as various squeeze oil film parameters have been obtained.

Notation

a - length of the crack, [m].
b - hertzian contact footprint half width, [m].
E' = equivalent Young modulus, [MPa] $E' = 2/[(1-\nu_1)^2/E_1 + (1-\nu_2)^2/E_2]$
F - normal load intensity, F= N/L, [N/m]
G - material parameter, $G = \alpha' E'$
H - EHD oil film thickness, [m].

h - squeeze oil film thickness, [m]
K_I - mode I stress intensity factor, [MPa $\sqrt{m}$].
K_I' - dimensionless mode I stress intensity factor, $K'_I = K_{II}/(p_0\sqrt{b})$
K_{II} - mode II stress intensity factor,[MPa $\sqrt{m}$].
K'_{II} - dimensionless mode II stress intensity factor, $K'_{II}= K_{II}/(p_0\sqrt{b})$
N - normal load, [N]
L - contact length, [m].
p, $\bar{p}$ -pressure in EHD and squeeze film, [MPa].
p_0 - maximum Hertz' contact pressure, [MPa].
R - roller radius, [m].
R' - equiv. radius of rollers, [m] $R'= R_1R_2/(R_1+R_2)$.
s, t - co-ordinate system attached to the crack tip, [m].
τ - time [sec].
u - velocity in 'x' direction , [m/s].
u' - av. entrainment rolling speed, [m/s] $u'= (u_1+u_2)/2$.
U - speed parameter, $U = \eta_0 u'/(E' R')$.
v - velocity in 't' direction [m/s].
W - load parameter, $W = F/(E'R')$.
α - angle of crack inclination, [°].
α' - piezocoefficient of oil viscosity, [Pa^{-1}]
γ - angle between crack faces, [°].
λ = traction to normal load ratio, $\lambda = q_0/p_0$.
μ - coefficient of friction between crack faces.
x, x' - co-ordinates, [m], $\bar{x} = x/b$
η_0 - oil viscosity in ambient conditions,[Pa s].
ρ - oil density [kg/m^3].
Indices:
1, 2 - for lower and upper surface, respectively.
a - for the point of the first pressure maximum.
b, e - for beginning and end of squeeze oil film

Introduction

The behaviour of a surface breaking rolling-contact fatigue crack, which is exposed to the pure elasto-hydro-dynamic lubrication (EHL) conditions is analysed. An influence of oil on the process of contact fatigue has been already pointed out in 1935 by S. Way [2], who observed the pits created even in fully developed EHD lubrication conditions, which prevents the interacting surfaces from metallic contacts. The theoretical 2D model

corresponding to the experiments of S. Way and Yamamoto [3] has been developed and used for numerical simulation of the crack propagation process by L. M. Keer and M. D. Bryant [4]. They analysed the surface breaking crack embedded in the elastic half-space taking into account friction between the crack faces and simulating the contact load by the Hertz pressure distribution. In their analysis the liquid interaction in the crack interior was modelled by assuming that the fluid lubricant transmits proportionally over the upper part of the crack the normal Hertzian contact pressure applied at the mouth of the crack. They obtained the stress intensities large enough to cause the crack growth and calculated pitting times on the basis of the Paris crack growth law, but they have not indicated the mechanism, which could be responsible for propagating contact fatigue cracks. Bower [5] used also the 2D model for his analysis, in which he examined the effect of the so called "fluid entrapment mechanism" on the values and histories of the stress intensity factors. He stated that such mechanism can take place, when the fluid is locked in the crack interior and pressurised by the contact load. The results obtained from the analysis seem to give an explanation for "the preferred" direction of cracks growth for the fluid entrapment mechanism, but these phenomena are not fully explained and require the modelling which take into account fluid mechanics.

Bogdański, Olzak and Stupnicki [6], applied 2D FEM model as a cylinder and prism for the analysis of liquid effects on the behaviour of surface breaking rolling contact fatigue cracks. They obtained normal and tangential contact interactions between the contacting bodies by means of solving the contact problems for the consecutive positions of cylinder rolling over the prism. Using the similar model, they investigated the fluid entrapment effect together with tractive force and residual stresses acting in the area of crack [7], [8]. These results were used in combination with an empirical crack propagation laws derived from experiments on rail steels under non-proportional mixed-mode I and II loading cycles [9] for evaluating the RCF crack growth rate and direction in rails.

A "body force method" have been developed by Murakami and Nasser [10], which was used in the analyses of three dimensional contact fatigue cracks by Kaneta and Murakami [11]. The results obtained from these analyses cover wide scope of cases, but again cracks are embedded in the elastic half - space and contact load is approximated by the Hertzian pressure.

The "squat" type of crack which occurs in rails has been modelled as a 3D real geometry object and analysed for the first time by Bogdafiski, Olzak and Stupnicki [6], [12]. They applied FEM model for a wheel and a section of rail containing the typical "squat" shape crack. They have solved a series of consecutive contact problems, which occur between rail and wheel during rolling of the wheel over the crack, with the use of the flexibility matrices and the iterative procedure. They found the significant differences between the contact pressure distributions obtained from the solution of the real geometry contact problem and those predicted by the Hertz' theory.

The analysis of rolling contact fatigue cracks in the conditions of elasto-hydro-dynamic lubrication have been attempted for the first time by Bogdafiski [13], who used the EHD pressure distribution in the 2D FE model for loading the crack. He investigated an influence of crack inclination angle and length, traction, as well as friction between the crack faces on the histories of the stress intensity factors during loading cycle. The states of crack opening, locking and sliding have been taken into account in the analysis. He carried out calculations for the corresponding cases with the Hertzian pressure distributions, and found that the EHD pressure profile used as crack load gives not only the different values of the SIFs, but also alters the nature of the phenomena occurring in the contact area. Bogdafiski and Brown [14] used the above mentioned results in combination with empirical crack propagation laws derived from experiments with non-proportional mixed-mode I and II loading cycles [15], [16], for evaluating the RCF crack growth rate and direction in EHL conditions. They found that the SIF ranges produced by the EHD normal and traction load applied to the surface of the member containing the crack, are not sufficient for driving the crack with the rate observed in practice. They concluded that either fluid pressure transmitted from the oil film to the crack interior or a kind of the another fluid action or both significantly enhance the fatigue mechanism in actual rolling contact applications.

Many of the results of the above discussed analyses can be successfully used for at least partial explanation of the phenomena occurring during cyclic loading of rolling contact fatigue cracks in gears, bearings and railway tracks. However, the particular contact couples have their specific features, which should be taken into consideration when more precise models are created. The contact of the two members separated by the EHD oil film is an example of such a couple. Due to the presence of the oil film, solving of

the contact problem is not necessary. Instead of this, the proper approach seems to be to apply the EHD pressure and traction distributions as the contact load. The continuous presence of oil in the contact area, and consequently in the vicinity of the crack mouth, when it is passing through this zone, creates conditions for the above mentioned enhancement of the discussed here mechanisms of crack propagation.
In this paper, the attempts are undertaken to model these mechanisms on the basis of fluid mechanics, and to account for the effects associated with fluid sucking in, and flowing out from the crack interior.

Modelling

The two-dimensional finite element model of a oblique, surface breaking crack has been applied to investigate the state of stress in the vicinity of a crack tip, during cyclic EHD contact loading. The EHD contact couple (Fig. 1a.) is modelled here as a prism with the length of 32b and height of 7b, which is subjected to the travelling EHD pressure and traction distributions (Fig. 1b.). One cycle of rolling in this system is equivalent to one passage of load. The loading cycle begins for the position of the load centre at $x = -5b$, and ends at $x = 7b$. The crack, is embedded in the middle of the prism, and is described by the length "a" and an angle of inclination to the horizontal "α". The crack mouth is located at $x = 0.0$. Fully developed EHD conditions have been assumed, which assure an existence of the continuous oil film, thick enough to prevent the contacting surfaces from touching each other. As an approximation of a real pressure and traction distributions acting in the EHD oil film, those of a numerical solution of thermo-elastohydrodynamic contact problem has been taken for the analysis, [1]. On the basis of linear fracture mechanics, values, ranges and histories of fluctuations of the stress intensity factors SIF; K_I, K_{II} at the crack tip are determined for the cycle of contact loading. Two different ways of oil interaction on the crack faces have been incorporated into the model. The first one accounts for the presence of the small amount of oil in the crack interior, which is sufficient for lubricating the crack faces and consequently reducing friction between them.

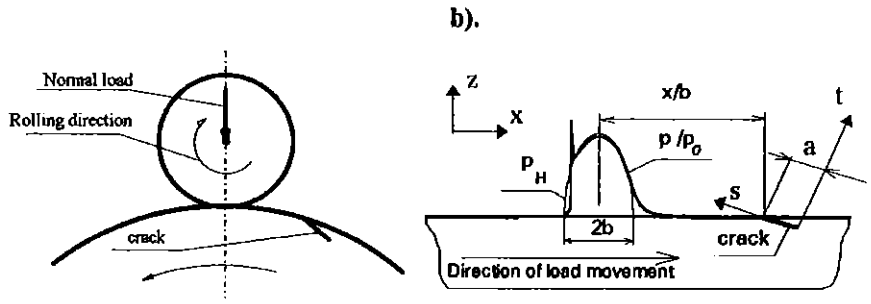

Fig. 1. a). EHD contact couple members, b). Crack geometry and load configuration.

In distinction from the case of flooded crack, this approach is called here the model for dry conditions.

The concept of a squeeze oil film build up between the crack faces, which is introduced for the first time here, is incorporated into the model as the mentioned above second way of oil interaction. This concept will be dealt with in the next Chapters.

The model for dry conditions.

It is assumed, that an amount of oil, which is present in the crack interior is not sufficient for transmitting the pressure from the EHD oil film nor for building up the squeeze film between the crack faces. The fluid entrapment effect is also not possible to develop in these conditions. In this model, the tangential and normal interactions between the crack faces are taken into account, and determined through the contact problem being subsequently solved during simulation of the cycle of loading. Three states of the crack faces interactions are distinguished; crack open, crack being in sticking contact and crack in sliding contact. This approach has been already explained and applied in [13], [14]. A number of results for this model have been already discussed in these papers.Some further analyses for loads, crack lengths and angles of inclination, which have not been published yet, will be discussed in this paper.

The model of a crack driven by the squeeze oil film.

The phenomena taking place in the crack loading process are very fast. In the common practical EHL applications like bearings and gears, the range of the speed parameter is $U \approx 10^{-11} \div 10^{-10}$, what yields, for the typical geometry, to the time necessary for the crack to travel through the contact load zone, which is of order of fractions of milliseconds. For the conditions analysed here, this time is equal to about 280 microseconds. The average distance between the crack faces is of order of fraction of micrometer. Hence, the layer of oil of the above mentioned thickness is squeezed between the crack faces during the cycle of loading. The parameters describing the crack behaviour, i. e. the time for which the crack is exposed to the load and the characteristic dimensions, such as the ratio of the crack length to the thickness of the clearance, which is of order of 10^3, are comparable to those of the "ball impact experiment" [17]. The total time of impact in this experiment was about 260 microseconds, during which the squeeze oil film was build up and the ball rebounded without touching the steel plate. On the basis of these similarities, it could be concluded that motion of the crack faces is governed by the squeeze oil film phenomena. Referring to the above an attempt of using the squeeze oil film model for describing the crack behaviour in EHL conditions have been undertaken.

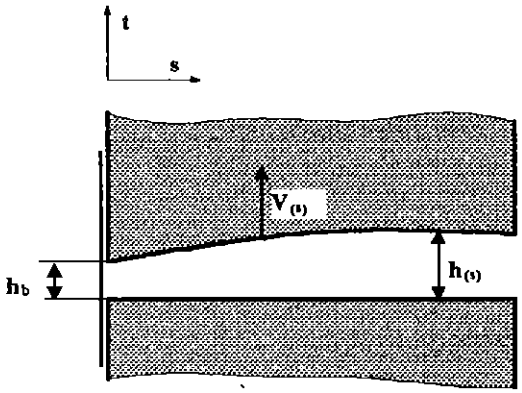

Fig. 2. The squeeze oil film configuration.

If the oil property variations across the oil film are neglected; $\frac{\partial \eta}{\partial t} = 0$; $\frac{\partial \rho}{\partial t} = 0$, the following form (1) of the Reynolds equation [18] can be used to describe the oil squeeze film of configuration shown in Fig. 2.

$$\frac{\partial}{\partial s}\left(\frac{\rho_{(s)} h_{(s)}^3}{12\eta_{(s)}}\frac{\partial p}{\partial s}\right) = h_{(s)}\frac{\partial \rho_{(s)}}{\partial \tau} + \rho_{(s)}\left(V_{2_{(s)}} - V_{1_{(s)}}\right) \qquad (1)$$

In general case, the solution of this equation requires the knowledge of the particular functions of he following variables: h, v_1, v_2, ρ, η, which are dependant on each other, and related to the external and internal pressure. Complexity of the problem is multiplied by the feedback between the EHD oil film operating outside the crack and the squeeze oil film, which controls the fluid flow inside the crack. Solution of the general case is beyond the scope of this paper, but some simplified considerations will be presented to demonstrate characteristic features of the squeeze oil film and its influence on the crack behaviour.

For the case of two parallel faces approaching each other with constant speed v, and for the steady state case, which means assuming the following; $\frac{\partial \rho}{\partial \tau} = 0$, $\frac{\partial h}{\partial s} = 0$,

equation (1), takes the form;

$$\frac{\partial}{\partial s}\left(\frac{\rho}{12\eta}\frac{\partial \bar{p}}{\partial s}\right) = \frac{1}{h^3}\rho \cdot v \tag{2}$$

After applying the Barus viscosity-pressure relationship; $\eta = \eta_o e^{\alpha' \bar{p}}$, the double integration with the first and second boundary conditions; $s = 0 \rightarrow \frac{\partial \bar{p}}{\partial s} = 0$ and $s = a \rightarrow \bar{p} = \bar{p}_e$ leads to the following expression for pressure distribution along the faces of the crack:

$$\bar{p}_{(s)} = -\frac{1}{\alpha'}\ln\left[e^{-\alpha' \bar{p}_e} - \alpha' \cdot q_{(s)}\right] \tag{3}$$

Where per analogy to the solution of the EHD contact problem 'q' is the so called "reduced pressure" which is defined here as:

$$q_{(s)} = \frac{6 \cdot v \cdot \eta_o}{h^3}\left(s^2 - a^2\right) \tag{4}$$

The results closer to reality can be obtained by approximating the squeeze oil film shape with the wedge having h_b thickness at its beginning (s=0) and an angle γ between the crack faces; $h_{(s)} = h_b + s \cdot \tan \gamma$. Applying the same as before procedure and assuming again constant speed v, the pressure distribution inside the crack can be expressed by the same as before equation (3) with the reduced pressure defined this time as follows:

$$q_{(s)} = \frac{12\, v \cdot \eta_o}{tg^2 \gamma}\left[\frac{h_b}{2}\left(\frac{1}{h_{(s)}^2} - \frac{1}{h_e^2}\right) + \left(\frac{1}{h_e} - \frac{1}{h_{(s)}}\right)\right] \tag{5}$$

For similar definition of the crack clearance shape, and for the upper crack face rotating as a rigid body with angular velocity ω the reduced pressure is :

$$q_{(s)} = \frac{6 \cdot \omega \cdot \eta_o}{tg^3 \gamma} \left[\left(\ln h_{(s)} - \ln h_e \right) + 2h_b \left(\frac{1}{h_{(s)}} - \frac{1}{h_e} \right) + \frac{h_b^2}{2} \left(\frac{1}{h_e^2} - \frac{1}{h_{(s)}^2} \right) \right] \qquad (6)$$

For the same as before oil film shape, and for the particular points of the upper crack face moving with the velocities defined according to the following function: $v_{(s)} = \omega \cdot s^2/a$, which makes the case more realistic, the pressure distribution along the crack length is described by equation (3) with the reduced pressure defined as follows:

$$q_{(s)} = \frac{4\eta_o \cdot \omega}{a \cdot tg^4 \gamma} \left\{ \left(h_{(s)} - h_e \right) + 3h_b \left(\ln h_e - \ln h_{(s)} \right) + h_b^2 \left[\frac{1}{h_e} \left(3 - \frac{h_b}{2h_e} \right) - \frac{1}{h_{(s)}} \left(3 - \frac{h_b}{2h_{(s)}} \right) \right] \right\} \qquad (7)$$

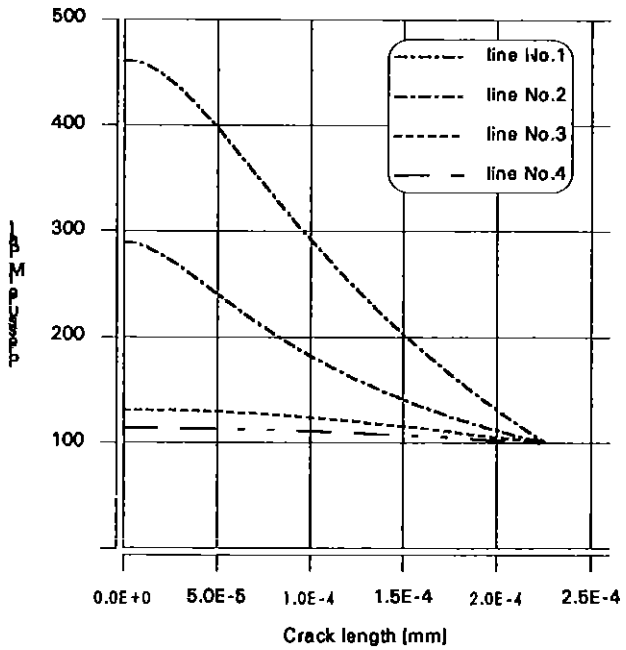

Fig. 3. Pressure distributions in the crack interior according to various models of the squeeze oil film, line No. 1 - eq. 4, No. 2- eq. 6, No. 3 -

The pressure distributions determined on the basis of the above developed models, for the exit pressure p_e=100 MPa and for the geometrical and oil parameters applied here, are shown in Fig. 3.

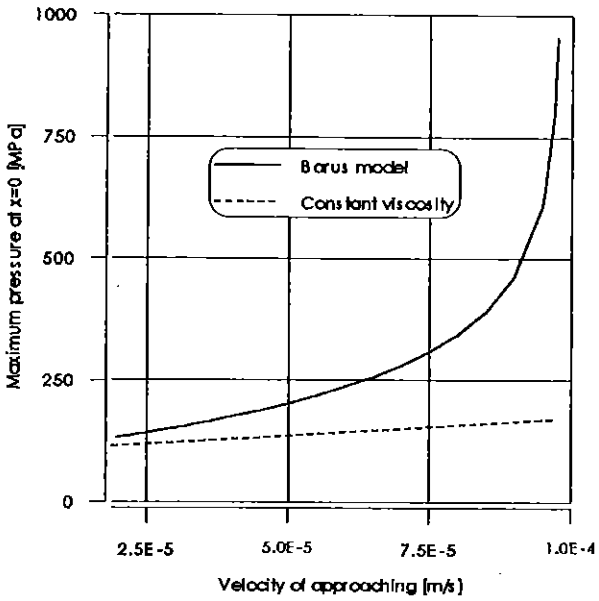

Fig. 4. The maximum oil pressure in the squeeze oil film (for s = 0) for the model described by equation (6).

Additionally, the curve No. 4 represents the case based on the model described by the function (6) with the assumption of constant viscosity. This diagram demonstrates how strongly the pressure distribution depends on the way of modelling of the squeeze oil film. The pressure distribution is also very sensitive to the variation of the speed of the faces approaching each other. This is shown in Fig. 4 as a values of the maximum pressure in the oil film (for s=0) against the speed of approaching bodies. As shown, the pressure in the oil film can attain high values for quite small approaching velocities.

For evaluating a possible effect of squeeze oil film action on the crack tip loading, the model described by equation (3) and (6) has been chosen, and the feedback between the EHD oil film at the surface, and squeeze oil film inside the crack has been taken into account. For each step of the FE analysis, the new EHD pressure distribution has been determined trough the full solution of the EHL contact problem [1], with the EHD oil clearance modified by the bump created by the crack. The pressure distribution inside the crack has been generated according to equation (3) with the reduced pressure defined in (6), taking into account the equilibrium conditions for the wedge shaped part of the prism located above the crack.

Results and discussion.

For each cycle of loading the state of stress in the vicinity of the crack tip has been determined and consequently the history diagrams of mode I and mode II Stress Intensity Factors (SIF) have been found. These diagrams are shown as the curves plotted for the particular SIF values against the position of the load centre. The history diagram for the mode I SIF shown in Fig. 5 has been chosen here to explain how to read such diagrams in this paper. The EHD pressure distribution marked in this figure as p/p_o is travelling from left to right, and its consecutive positions are described by the co-ordinate x/b, which is the distance between the centre of the pressure distribution and the crack mouth. For each position of this load the SIFs at the crack tip are determined and plotted against these positions.

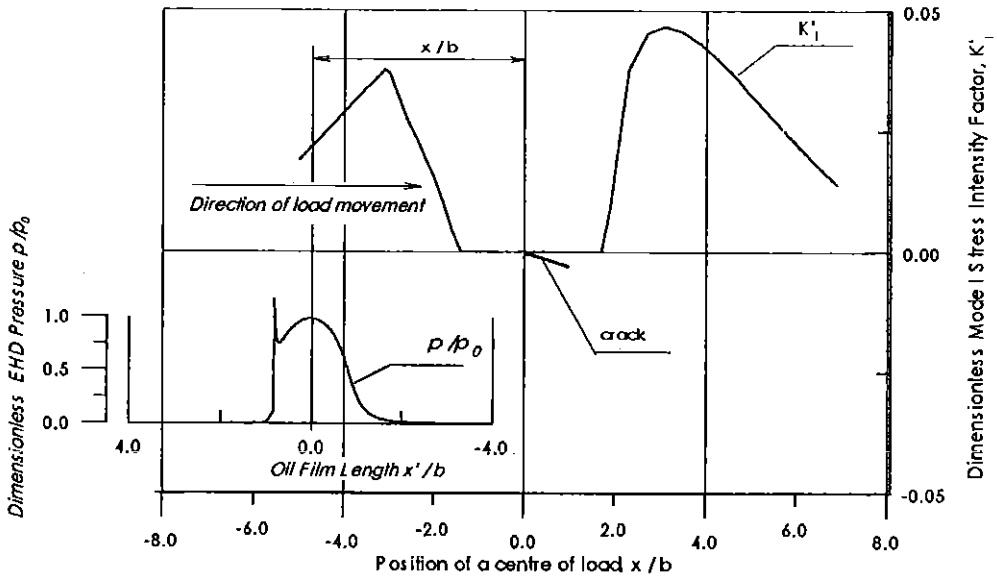

Fig. 5. An example of the history diagram for the dimensionless Mode I Stress Intensity Factor at the crack tip for the EHD pressure distribution p/p_o travelling from left to right along the co-ordinate x/b.

The above described system of presentation is used for both the results obtained from analyses carried out for dry conditions and those of the squeeze oil film.

The cases for dry conditions.

Most of the results for dry conditions for the range of crack slopes form 25° to 60° have been presented and discussed in [13] and [14]. Some new cases for smaller angle of crack inclination, i. e. for $\alpha = 15°$ for various friction coefficients between the crack faces, and for larger contact load will be presented here and compared with the squeeze oil film cases. Apart from the history diagrams, it is interesting to see the history of crack behaviour during the cycle of loading. Such history includes the phases of crack opening and locking, with the sticking or slipping contact between its faces being distinguished. The typical example of such diagrams for dry conditions is shown in Fig. 6, in which the shape of the crack is presented in exaggerated scale for its eight characteristic positions. The state of the crack faces is also marked in these diagrams with the numbers, whose minings are explained in the figure caption.

Figure 6a shows the crack at the beginning of the loading cycle for the co-ordinate $x/b = -5.0$. As shown, the crack is open on its whole length. Figure b) corresponds to the position of the crack at the edge of the load zone. Starting form the position just after the edge of the load zone, for which the crack is shown in Fig c) the crack is gradually closing, what is demonstrated in Fig. d), e), and f). Fig. 6 g) shows the crack for the position after leaving the load area. At this position, the upper part of the prism above the crack is unloaded, what produces the maximum opening of the crack within the whole cycle. The last figure h) corresponds to the end of loading cycle, for which the crack is at the distance of $x/b = 4.7$ from the centre of load.

The histories of the mode I and II stress intensity factors for the above discussed crack for various friction coefficients between the crack faces are presented in Fig. 7. As shown, the range of the mode II SIF variation depends strongly on friction between the crack faces. The parts of the cycles, for which the crack faces are locked are clearly shown here as the horizontal sections of curves. The corresponding histories of the mode I SIFs do not depend much on friction between the crack faces. The curves for particular friction coefficients are very close to each other. The section of the curve, for which the SIF K'_I is equal to zero corresponds to the part of the cycle, during which the crack is closed. The exemplary comparison of the mode I and II SIFs histories for two various lengths of the

crack is shown in Fig. 8. The cycles are similar to each other in respect of shape, but the range of the mode II SIF is much higher for longer crack.

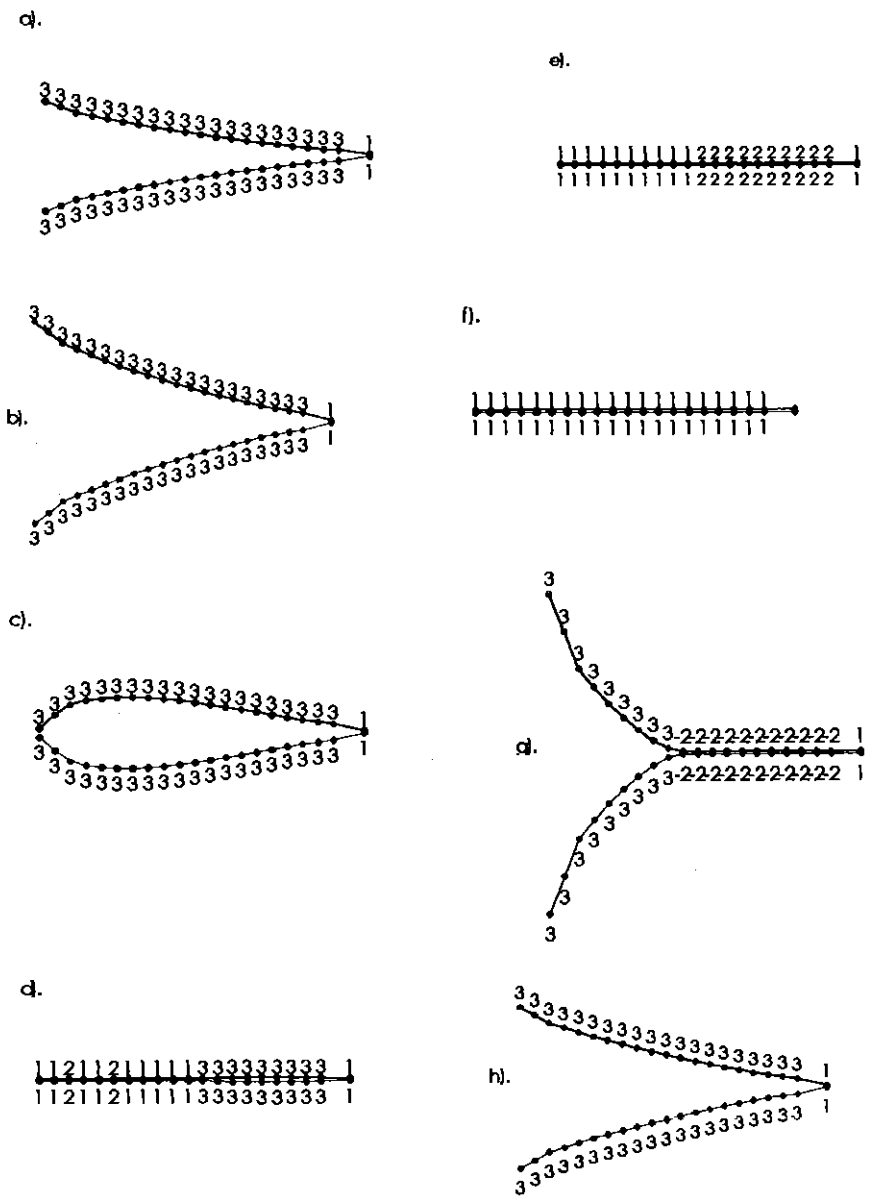

Fig. 6. The shapes of the crack for various positions of load during loading cycle, dry conditions. Loads: $p_0 = 903.1$ Mpa, $\mu = 0.2$, $\alpha = 15°$, $\lambda = 0.056$. '1' – crack locked, '2'– crack faces slip in clockwise direction, '–2'– crack faces slip in counterclockwise direction, '3' –crack open. a). $\bar{x} = -5.0$, b). $\bar{x} = -3.1$, c). $\bar{x} = -3.0$, d). $\bar{x} = -1.8$, e). $\bar{x} = -1.0$, f). $\bar{x} = 0.7$, g). $\bar{x} = 1.3$, h). $\bar{x} = 4.7$.

The ranges of the SIF K_{II} for coefficient of friction equal zero are the highest ones from the whole set of cases analysed. But for the practical EHL applications analysed here, i. e. for b = 0.226 mm, even the ranges for frictionless cases, are not sufficient for exceeding the LEFM threshold and causing the crack growth

The crack propagation estimates for EHL conditions have been made by Bogdański and Brown [14] with the use of empirical models developed for mixed-mode growth mechanisms by Wong at al [15] and Brown at al [16]. The reasonably low propagation rates have been obtained only after scaling the analysed geometry, with the use of rules of dimensional analysis, to model the crack length of 5.08 mm, which is comparable to many rail/wheel contact cracks found in practice. However, in bearings and gears fatigue damage is observed in practice, and in rails growth rates can be about 100 times faster than those predicted there. Considering this, they came to the conclusion, that either the fluid pressure in the crack, or another fluid action or both, significantly enhance the fatigue mechanism in actual rolling contact applications. Referring to this, an attempt has been undertaken to model liquid interaction in the crack interior using for the first time the concept of the squeeze oil film build between the crack faces.

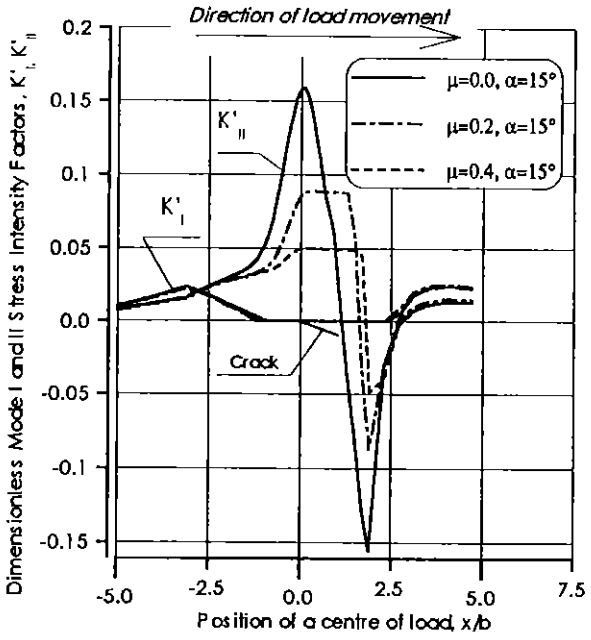

Fig. 7. The history diagrams for the mode I and II stress intensity factors, p_0 = 903.1 Mpa, α = 15°, λ = 0.056, a/b=1.0, dry conditions.

The results obtained from the analysis based on this model will be dealt with in the next Chapter.

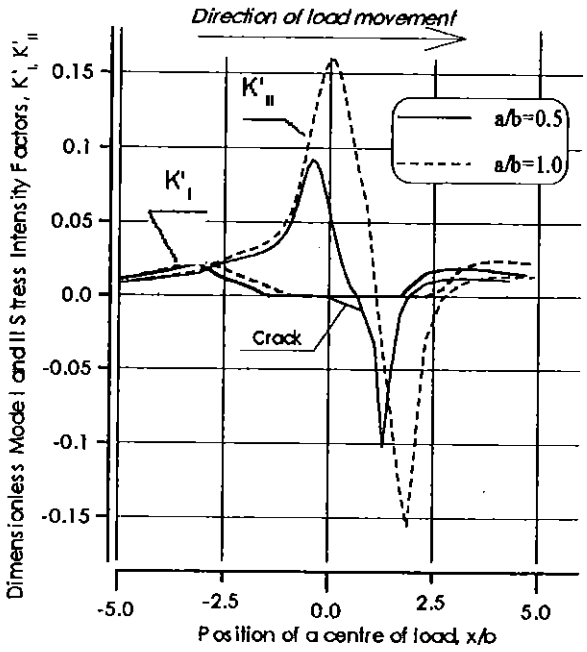

Fig. 8. Comparison of the SIFs for two crack lengths, p_0 = 638 MPa, α =15°, λ = 0.056, μ_* =0.0.

The squeeze oil film conditions.

To understand the feedback between the crack behaviour and the EHD oil film existing in the EHL contact zone, it is necessary to realise the specific features of the fluid flow between the contacting surfaces. This is the low Reynolds number flow, under extremely high pressure and shearing forces, which is very sensitive to the changes of the height of the flow channel bounded by the solid surfaces. This sensitivity is extremely high in the centre region of the contact zone, where the pressure attains the maximum values and film thickness its minimum ones. It means, that very tiny change in the film thickness or its gradient along the crack length in this region, (caused for instance by the change of the shape of bounding surfaces.) causes enormous changes in the pressure values and gradients. This characteristic feature of the EHD oil film can be concluded from the nature of the Reynolds equation, which governs the oil flow in this region, [18].. In such conditions, any shape irregularity (bump, dent, wave, pocket or valley) causes pressure fluctuations if it enters the EHD contact zone. In particular, a bump in the form of lifted

up part of the material above the crack can cause significant local pressure rise. This irregularity of the oil film boundary is exposed to the high pressure, which causes the crack to tend to close, what eventually leads to the squeeze oil film effect between the crack faces. The intensity of this phenomena depends strongly on the position of crack in relation to the load, what is illustrated in Fig. 9. In this figure, the pressure distribution and EHD oil film shape determined from the full solution of the EHD contact problem, with the use of algorithm described in [1], are plotted against the length of the oil film, for the crack mouth located at $x/b = -1.0$ and $x/b = -0.6$, respectively. The local pressure ripples, shown in these figures do not close the crack immediately, despite their significant height, due to the opposite action of the squeeze oil film, which is very sensitive to the clearance height and the velocity of bounding surfaces in the similar way as the EHD oil film. This combined action of external and internal fluid films creates conditions not only for transmitting the oil pressure from the EHD oil film to the crack interior, but also for producing an extra pressure rise along the crack. As a result, the pressure acting on the crack faces can be in certain conditions even higher then the pressure at the crack mouth. The results of the FE analysis taking into account the above mentioned effects are shown in the form of the SIF K'_I and K'_{II} histories in Fig. 10. As shown, the squeeze oil film action has the greatest effect on the range of the SIF K'_I. In this particular case, the discussed range increased due to this action more than 32 times. Simultaneously, the cycle of the mode II SIF has altered its shape, undergoing the change of shearing direction two times during the loading period, with the 130 % rise of the range.

a).

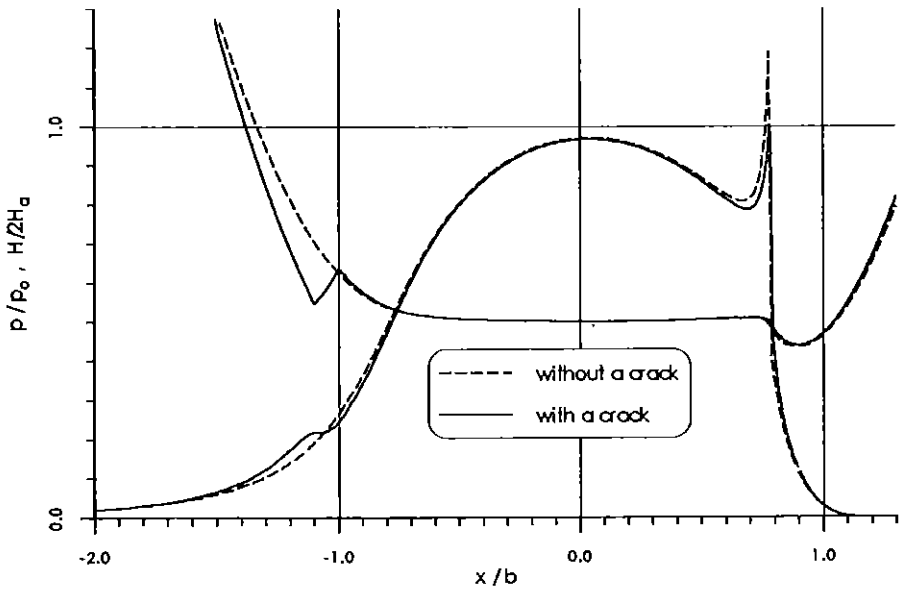

b).

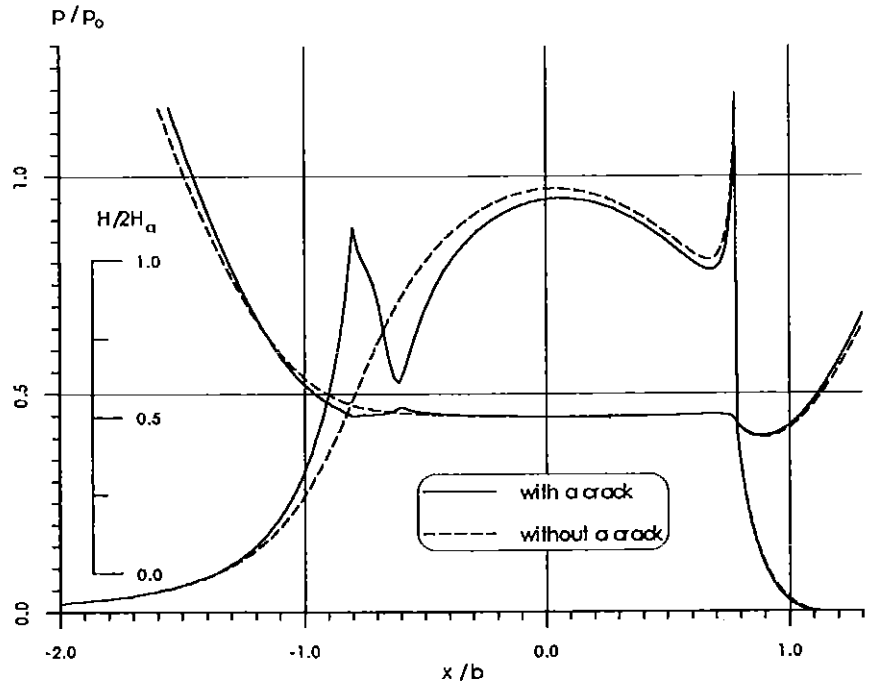

Fig. 9. Pressure distribution and EHD oil film shape for the squeeze oil film conditions, p_0 = 903.1 MPa, α =15°, λ = 0.056, a/b=1.0, crack mouth located at:

a). x/b = – 1.0 b). x/b = – 0.6.

a).

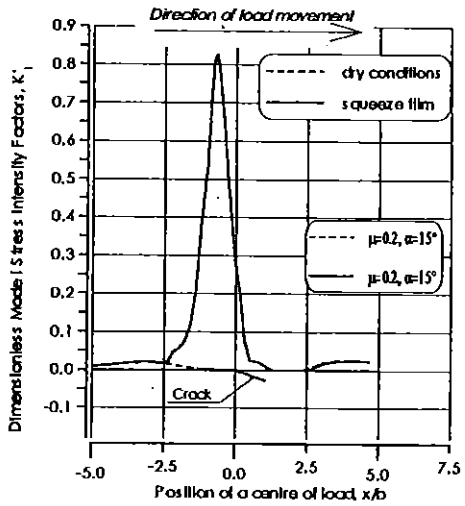

b).

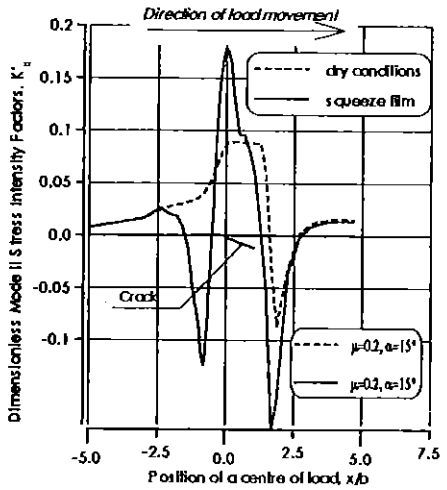

Fig. 10. Comparison of the SIF histories during loading cycle for the crack driven by the squeeze oil film and for the case of dry conditions, $p_0 = 903.1$ MPa, $\alpha = 15°$, $\lambda = 0.056$, a/b=1.0. a). Mode I SIFs; b). Mode II SIFs.

The characteristic horizontal section of the cycle curve typical for the period of sticking contact between the crack faces, does not exists any more for the case with the squeeze oil film action. This is presumably caused by the pressure acting on the crack faces, which keeps them in distance and cancels the friction effects. Applying empirical crack growth models, the same as mentioned in the previous chapter, gives a reasonable coplanar crack growth rate of order of 5.0 nm/cycle, which implies life of about $10^7 \div 10^8$ cycles to failure.

The change of shearing direction shown in Fig. 10b. is caused by the squeeze oil film pressure, which supports the upper face of the crack preventing it from slipping down along the fracture plane under the pressure of the inlet part of EHD film.

Conclusions.

Finite element solutions for the crack exposed to the cyclic load in EHL conditions can be successfully used for determining the histories of stress intensity factors, which are in combination with the empirical laws derived from fatigue experiments the data for predicting the crack growth rates and direction. The classical approach accounting only for lubrication of crack faces does not provide the explanation for observed in practice fatigue contact damage. The ranges of stress intensity factors obtained from such analyses are not sufficient for exceeding the LEFM threshold. The mechanism of interaction between the EHD oil film and the squeeze oil film keeping the crack faces apart, introduced in this paper, provides satisfactory explanation for the rate and direction of the crack growth observed in practice. In the conditions of permanent presence of oil, which exist in EHD contact area, there are the periods of loading cycle, in which the crack can be filled up with oil, and then during passing through the high pressure region, this oil is squeezed between the crack faces. Squeezing crates pressure rise along the crack, from the exit pressure at the crack mouth to its maximum value in the vicinity of the crack tip. The shallow angle of the cracks growth, which is also observed in practice can be explained on the ground of the feedback between the EHD oil film existing between contacting surfaces and the squeeze oil film acting between the crack faces. This feedback involves the distortion of the EHD oil film shape caused by the pressure of liquid contained in the crack interior. A part of the surface located directly above the crack is displaced outwards, in the form of a bump, udder the pressure exerted on the crack faces by the squeeze oil film. This results in the feedback action of the pressure ripple build up in the EHD oil film by the presence of the bump. Such interaction is especially intensive for the shallow angle cracks.

References

(1) Bogdański, S., Paturski, Z. & Wolff, R., (1992). Numerical solution to the thermal EHD line contact problem. *Archive of Machine Design* 40 (2):pp. 155-182.

(2) Way, S., (1935). Pitting due to rolling contact. *J. App. Mech., Trans. ASME* 2, 49-58.

(3) Yamamoto, T., (1980) Crack Growth in Lubricating Rollers, *Solid Contact and Lubrication*, Ed. H. S. Cheng and L. M. Keer, ASME AMD, Vol. 39, pp. 223 - 236.

(4) Keer, L. M. & Bryant, M. D., (1983). A pitting model for rolling contact fatigue. *J. Lubr. Technol., Trans. ASME* 105: pp. 198-205.

(5) Bower, A. F., (1988). The influence of crack face friction and trapped fluid on surface initiated rolling contact fatigue cracks. *J. Tribology, Trans. ASME*, 110: pp. 704-711.

(6) Bogdański, S., Olzak, M. & Stupnicki, J., (1996). Numerical stress analysis of rail rolling contact fatigue cracks. *Wear* 191: pp. 14-24.

(7) Bogdański, S., Olzak M. & Stupnicki, J., (1996). Influence of liquid interaction on propagation of rail rolling contact fatigue cracks. *Proceedings of the 2nd mini conference on contact mechanics and wear of rail/wheel systems, Budapest*, 29-31 July, 1996, pp. 134-143.

(8) Bogdański, S., Olzak, M. & Stupnicki, J. (1993). An effect of internal stress and liquid pressure on crack propagation in contact area. *Proceedings of the 6th Congress on Tribology - Eurotrib '93, Budapest* 30 Aug.-2 Sept. 1993. Vol. 5: pp. 310-315.

(9) Bogdański, S., Stupnicki, J., Brown, M. W. and Cannon D. F., (1997). A two dimensional analysis of mixed-mode rolling contact fatigue crack growth in rails. Paper submitted to the *"5th International Conference on Biaxial/Multiaxial Fatigue & Fracture", Cracow (Poland), 8-12 September, 1997.*

(10) Murakami, Y. and Nemat - Nasser, S., (1983). Growth and stability of interacting surface flaws of arbitrary shape, *Eng. Fract. Mechanics*, Vol. 17, No. 3, pp. 193 - 210.

(11) Kaneta, M. & Murakami, Y., (1991). Propagation of semi-elliptical surface cracks in lubricated rolling/sliding elliptical contacts. *J. Trib., Trans. ASME* 113: pp. 270-275.

(12) Bogdański, S., Olzak, M. & Stupnicki, J., (1996). The effects of face friction and tractive force on propagation of 3D 'squat' type of rolling contact fatigue crack. *Proceedings of the 2nd mini conference on contact mechanics and wear of rail/wheel systems, Budapest*, 29-31 July, 1996, pp. 164-173.

(13) Bogdański, S., (1996). Finite element modelling of surface fatigue crack in EHD contact. To be published in the *Proceedings of the 3rd international Leeds-Lyon symposium on tribology, Leeds* 10-12 Sept. 1996.

(14) Bogdański, S., Brown, M. W., (1997). Modelling of surface fatigue crack growth in EHD contact. To be published in the *Proceedings of the International Conference "Engineering Against Fatigue" Sheffield (UK), 17-21 March, 1997.*

(15) Wong, S. L., Bold, P. E., Brown, M. W. & Allen, R. J., (1996). A branch criterion for shallow angled rolling contact fatigue cracks in rails. *Wear* 191: pp. 45-53.

(16) Brown, M. W., Hemsworth, S., Wong, S. L. & Allen, R. J., (1996). Rolling contact fatigue crack growth in rail steel. *Proceedings of the 2nd mini conference on contact mechanics and wear of rail/wheel systems, Budapest*, 29-31 July, 1996, pp. 144-153.

(17) Safa, M. M. A., Gohar, R., (1986), Pressure distribution under a ball impacting a thin lubricant layer. *Trans. of ASME. Journal of Lub. Technology* 108, pp. 372-376.

(18) Dowson, D., (1961), A generalised Reynolds equation for fluid lubrication, *Int. J. Mech. Sci., Pergamon Press Ltd, Vol. 4:*, pp. 159-170.